

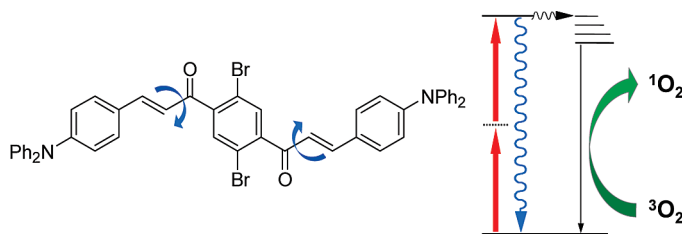
## Molecular Tuning of Phenylene-Vinylene Derivatives for Two-Photon Photosensitized Singlet Oxygen Production

Christian B. Nielsen,<sup>†,‡</sup> Jacob Arnbjerg,<sup>†</sup> Mette Johnsen,<sup>†</sup> Mikkel Jørgensen,<sup>‡</sup> and Peter R. Ogilby<sup>\*,†</sup>

<sup>†</sup>Center for Oxygen Microscopy and Imaging, Department of Chemistry, Aarhus University, Århus DK-8000, Denmark, and <sup>‡</sup>Polymer Department, Risø National Laboratory, DK-4000 Roskilde, Denmark

progilby@chem.au.dk

Received September 21, 2009



Substituent-dependent features and properties of the sensitizer play an important role in the photosensitized production of singlet oxygen,  $O_2(a^1\Delta_g)$ . In this work, we systematically examine the effect of molecular changes in the sensitizer on the efficiency of singlet oxygen production using, as the sensitizer, oligophenylene-vinylene derivatives designed to optimally absorb light in a nonlinear two-photon process. We demonstrate that one cannot always rely on rule-of-thumb guidelines when attempting to construct efficient two-photon singlet oxygen sensitizers. Rather, as a consequence of behavior that can deviate from the norm, a full investigation of the photophysical properties of the system is generally required. For example, it is acknowledged that the introduction of a ketone moiety to the sensitizer chromophore often results in more efficient production of singlet oxygen. However, we show here that the introduction of a carbonyl into a given phenylene-vinylene can, rather, have adverse effects on the yield of singlet oxygen produced. Using these molecules, we show that care must also be exercised when using qualitative symmetry-derived arguments to predict the relationship between one- and two-photon absorption spectra.

### Introduction

The photosensitized production of singlet molecular oxygen,  $O_2(a^1\Delta_g)$ , is a topic that has seen a great deal of attention over the last 40 years. Interest in singlet oxygen is broad-based, reflecting its importance in disciplines that range from synthetic organic chemistry<sup>1</sup> to photoinduced cell death.<sup>2</sup> Singlet oxygen is conveniently produced in a photosensitized process wherein a light-absorbing molecule (the so-called sensitizer) transfers its energy of excitation to ground state oxygen,  $O_2(X^3\Sigma_g^-)$ , (Figure 1). This process of energy transfer occurs most efficiently from the comparatively long-lived, lowest energy triplet state ( $T_1$ ) of the sensitizer.<sup>3</sup>

Over the years, a great deal of information has been accumulated regarding features of a sensitizer that result in the efficient production of singlet oxygen upon the absorption of a single photon (i.e., experiments performed in the domain where light absorption scales linearly with the incident power).<sup>3</sup> It has been shown, however, that singlet oxygen can also be formed upon two-photon absorption of a sensitizer (Figure 1)<sup>4–6</sup> and that the near-IR singlet oxygen phosphorescence thus produced can be used to accurately quantify the two-photon absorption cross section,  $\delta$ , of the sensitizer.<sup>7</sup> In turn, this has initiated a flurry of

(1) Clennan, E. L.; Pace, A. *Tetrahedron* **2005**, *61*, 6665–6691.  
(2) Redmond, R. W.; Kochevar, I. E. *Photochem. Photobiol.* **2006**, *82*, 1178–1186.  
(3) Schweitzer, C.; Schmidt, R. *Chem. Rev.* **2003**, *103*, 1685–1757.

(4) Frederiksen, P. K.; Jørgensen, M.; Ogilby, P. R. *J. Am. Chem. Soc.* **2001**, *123*, 1215–1221.

(5) Frederiksen, P. K.; McIlroy, S. P.; Nielsen, C. B.; Nikolajsen, L.; Skovsen, E.; Jørgensen, M.; Mikkelsen, K. V.; Ogilby, P. R. *J. Am. Chem. Soc.* **2005**, *127*, 255–269.

(6) Karotki, A.; Kruk, M.; Drobizhev, M.; Rebane, A.; Nickel, E.; Spangler, C. W. *IEEE J. Selected Top. Quantum Electron.* **2001**, *7*, 971–975.

(7) Arnbjerg, J.; Johnsen, M.; Frederiksen, P. K.; Braslavsky, S. E.; Ogilby, P. R. *J. Phys. Chem. A* **2006**, *110*, 7375–7385.

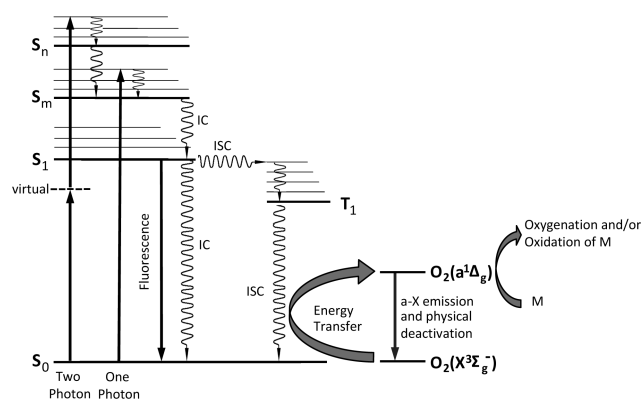


**FIGURE 1.** Illustration of one- and two-photon triplet-state photosensitized production of singlet oxygen,  $O_2(a^1\Delta_g)$ . Depending on the sensitizer, the simultaneous absorption of two photons may or may not populate the same state as that created upon the absorption of a single higher energy photon. ISC denotes intersystem crossing, and IC denotes internal conversion. The label “a-X emission” refers to the 1270 nm phosphorescence of singlet oxygen.

studies designed to elucidate features of a given molecule that optimize singlet oxygen production in this process where light absorption scales quadratically with the incident power.<sup>8–15</sup> One attribute of the latter nonlinear phenomenon is that the volume of excitation, and hence volume of singlet oxygen production, can be localized to a small spatial domain which can be advantageous in applications ranging from imaging to spatially selective chemistry.<sup>16,17</sup>

The nonlinear optical properties of oligo phenylene-vinylenes (OPVs) have been widely studied, and it is acknowledged that many molecules from this class of compounds can have large two-photon absorption cross sections.<sup>18–20</sup> Over the years, many groups have focused on elucidating key molecular features in OPVs that result in large values

of  $\delta$ .<sup>18–22</sup> Much of the discussion has focused on the architecture conducive to the facile intramolecular redistribution of electron density. The key underlying principle here is that, with the redistribution of large amounts of charge over a comparatively large intramolecular distance, one can increase the magnitude of the transition dipole moment and, in turn, increase the transition probability as manifested in a larger value of  $\delta$ .<sup>18,21,23,24</sup> Molecular features that can significantly influence the intramolecular distribution of charge include the judicious placement of electron donor and acceptor groups on a conjugated framework of extended length. As one might expect, molecular properties that depend on the transfer and localization of charge should likewise be quite susceptible to the effect of the surrounding solvent. In this regard, it is somewhat surprising that only few systematic attempts have been made to correlate observed  $\delta$ -values to changes in solvent.<sup>25–27</sup> We have shown that the OPV scaffold can be used in the development of both hydrophobic and hydrophilic two-photon singlet oxygen sensitizers.<sup>5,7,8,28</sup>

Principles of molecular design known to be beneficial for producing large two-photon transition probabilities are often undesired in terms of optimizing the photosensitized production of singlet oxygen (i.e., features that result in large values of  $\delta$  often result in small values of the quantum yield of singlet oxygen production,  $\Phi_{\Delta}$ ).<sup>5,8,28</sup> In particular, the extent of charge-transfer (CT), both within the sensitizer itself (i.e., intramolecular CT) as well as in the sensitizer–oxygen complex (i.e., intermolecular CT), can have a large adverse effect on the efficiency with which singlet oxygen is generated.<sup>3,29–33</sup> In general, CT character in a sensitizer and/or sensitizer–oxygen complex facilitates nonradiative deactivation of the excited state at the expense of energy transfer from the sensitizer to produce singlet oxygen. However, as mentioned previously, a high degree of intramolecular CT is desirable for obtaining large  $\delta$  values. Therefore, developing a sensitizer that is both a good two-photon absorber as well as an efficient singlet oxygen generator requires delicate balancing of the photophysical consequences of a change in the molecular architecture. In this argument, we assume that the extent of intermolecular CT in the sensitizer–oxygen complex will be larger for a sensitizer with a proclivity for

(8) Nielsen, C. B.; Johnsen, M.; Arnbjerg, J.; Pittelkow, M.; McIlroy, S. P.; Ogilby, P. R.; Jørgensen, M. *J. Org. Chem.* **2005**, *70*, 7065–7079.

(9) Arnbjerg, J.; Paterson, M. J.; Nielsen, C. B.; Jørgensen, M.; Christiansen, O.; Ogilby, P. R. *J. Phys. Chem. A* **2007**, *111*, 5756–5767.

(10) Arnbjerg, J.; Jiménez-Banzo, A.; Paterson, M. J.; Nonell, S.; Borrell, J. I.; Christiansen, O.; Ogilby, P. R. *J. Am. Chem. Soc.* **2007**, *129*, 5188–5199.

(11) McIlroy, S. P.; Cló, E.; Nikolajsen, L.; Frederiksen, P. K.; Nielsen, C. B.; Mikkelsen, K. V.; Gothelf, K. V.; Ogilby, P. R. *J. Org. Chem.* **2005**, *70*, 1134–1146.

(12) Oar, M. A.; Serin, J. M.; Dichtel, W. R.; Fréchet, J. M. J.; Ohulchanskyy, T. Y.; Prasad, P. N. *Chem. Mater.* **2005**, *17*, 2267–2275.

(13) Drobizhev, M.; Stepanenko, Y.; Dzenis, Y.; Karotki, A.; Rebane, A.; Taylor, P. N.; Anderson, H. L. *J. Phys. Chem. B* **2005**, *109*, 7223–7236.

(14) Andrasik, S. J.; Belfield, K. D.; Bondar, M. V.; Hernandez, F. E.; Morales, A. R.; Przhonska, O. V.; Yao, S. *ChemPhysChem* **2007**, *8*, 399–404.

(15) Belfield, K. D.; Bondar, M. V.; Hernandez, F. E.; Masunov, A. E.; Mikhailov, I. A.; Morales, A. R.; Przhonska, O. V.; Yao, S. *J. Phys. Chem. C* **2009**, *113*, 4706–4711.

(16) Skovsen, E.; Snyder, J. W.; Ogilby, P. R. *Photochem. Photobiol.* **2006**, *82*, 1187–1197.

(17) Collins, H. A.; Khurana, M.; Moriyama, E. H.; Mariampillai, A.; Dahlstedt, E.; Balaz, M.; Kuimova, M. K.; Drobizhev, M.; Yang, V. X. D.; Phillips, D.; Rebane, A.; Wilson, B. C.; Anderson, H. L. *Nat. Photonics* **2008**, *2*, 420–424.

(18) Albota, M.; Beljonne, D.; Brédas, J.-L.; Ehrlich, J. E.; Fu, J.-Y.; Heikal, A. A.; Hess, S. E.; Kogej, T.; Levin, M. D.; Marder, S. R.; McCord-Maughon, D.; Perry, J. W.; Röckel, H.; Rumi, M.; Subramaniam, G.; Webb, W. W.; Wu, X.-L.; Xu, C. *Science* **1998**, *281*, 1653–1656.

(19) Pond, S. J. K.; Rumi, M.; Levin, M. D.; Parker, T. C.; Beljonne, D.; Day, M. W.; Brédas, J.-L.; Marder, S. R.; Perry, J. W. *J. Phys. Chem. A* **2002**, *106*, 11470–11480.

(20) Strehmel, B.; Sarker, A. M.; Detert, H. *ChemPhysChem* **2003**, *4*, 249–259.

(21) He, G. S.; Tan, L.-S.; Zheng, Q.; Prasad, P. N. *Chem. Rev.* **2008**, *108*, 1245–1330.

(22) Terenziani, F.; Katan, C.; Badaeva, E.; Tretiak, S.; Blanchard-Desce, M. *Adv. Mater.* **2008**, *20*, 4641–4678.

(23) Mongin, O.; Porres, L.; Moreaux, L.; Mertz, J.; Blanchard-Desce, M. *Org. Lett.* **2002**, *4*, 719–722.

(24) Bischel, W. K.; Kelly, P. J.; Rhodes, C. K. *Phys. Rev. A* **1976**, *13*, 1817–1828.

(25) Johnsen, M.; Ogilby, P. R. *J. Phys. Chem. A* **2008**, *112*, 7831–7839.

(26) Woo, H.-Y.; Liu, B.; Kohler, B.; Korystov, D.; Mikhailovsky, A.; Bazan, G. C. *J. Am. Chem. Soc.* **2005**, *127*, 14721–14729.

(27) Toro, C.; De Boni, L.; Yao, S.; Belfield, K. D.; Hernandez, F. E. *J. Phys. Chem. B* **2008**, *112*, 12185–12190.

(28) Johnsen, M.; Paterson, M. J.; Arnbjerg, J.; Christiansen, O.; Nielsen, C. B.; Jørgensen, M.; Ogilby, P. R. *Phys. Chem. Chem. Phys.* **2008**, *10*, 1177–1191.

(29) Kristiansen, M.; Scurlock, R. D.; Iu, K.-K.; Ogilby, P. R. *J. Phys. Chem.* **1991**, *95*, 5190–5197.

(30) McGarvey, D. J.; Wilkinson, F.; Worrall, D. R.; Hobley, J.; Shaikh, W. *Chem. Phys. Lett.* **1993**, *202*, 528–534.

(31) Flors, C.; Ogilby, P. R.; Luis, J. G.; Grillo, T. A.; Izquierdo, L. R.; Gentili, P.-L.; Bussotti, L.; Nonell, S. *Photochem. Photobiol.* **2006**, *82*, 95–103.

(32) Arnbjerg, J.; Johnsen, M.; Nielsen, C. B.; Jørgensen, M.; Ogilby, P. R. *J. Phys. Chem. A* **2007**, *111*, 4573–4583.

(33) Jensen, P.-G.; Arnbjerg, J.; Tolbod, L. P.; Toftgaard, R.; Ogilby, P. R. *J. Phys. Chem. A* **2009**, *113*, 9965–9973.



**FIGURE 2.** General OPV structure where X denotes the moiety in which systematic molecular changes were made.

intramolecular CT (i.e., intermolecular CT to yield a Sens-O<sub>2</sub> state with Sens<sup>+</sup>·O<sub>2</sub><sup>-·</sup> character will more readily occur for a sensitizer with an electron-donating moiety).<sup>29–33</sup>

Although general features of a molecule that give rise to large values of  $\delta$  do not often give rise to large values of  $\Phi_{\Delta}$ , exceptions to this “rule” exist.<sup>10,13,17</sup> With this in mind, it is now necessary to embark on a series of more methodical and systematic studies to elucidate molecular features of a chromophore that can concomitantly result in large values of  $\delta$  and  $\Phi_{\Delta}$ . In the final analysis, it is the magnitude of the product  $\delta\Phi_{\Delta}$  that carries meaning in characterizing the efficiency of a two-photon singlet oxygen sensitizer. To this end, we set out to examine the effects of systematically adding/deleting specific functional groups in a given sensitizer system. To establish continuity with published data, we felt it would be beneficial to work with a specific OPV framework with diphenylamino groups at both ends of the chromophore (Figure 2).

## Results and Discussion

Our starting point in this study was the dibromo OPV **2** (Figure 3). This compound produces singlet oxygen in moderate yield and has a reasonably large  $\delta$  value.<sup>7</sup> Relative to the corresponding OPV that lacks the Br substituents, the presence of these heavy atoms in **2** boosts the efficiency of S<sub>1</sub> → T<sub>1</sub> intersystem crossing which, in turn, results in the more efficient production of singlet oxygen (Figure 1).<sup>11</sup>

In addition to the above-mentioned internal heavy atom effect, another well-known approach to facilitate S<sub>1</sub>–T<sub>1</sub> intersystem crossing is to introduce carbonyl moieties into the chromophore (El-Sayed’s Rules).<sup>34</sup> As such, some of the best known and most efficient singlet oxygen sensitizers are ketone-containing molecules.<sup>35</sup> We expected that the symmetrical addition of two carbonyl moieties to the chromophore in **2** might be advantageous in two ways: (1) we could increase the efficiency of intersystem crossing to the triplet state and, as such, increase the singlet oxygen yield, and (2) we could increase the extent of intramolecular charge redistribution which would be manifested in a larger value of  $\delta$ . Thus, we first chose to examine the behavior of compound **1** (Figure 3) and compare this to compound **2**.

In conjunction with the detailed study of **1** and **2**, we set out to use our OPV system to systematically examine the effects of (1) changing the substituents on the central aromatic ring and (2) changing the central aromatic ring itself. The intent here was to establish a broader database upon which substantive and compelling general conclusions could be drawn.

**1. Comparing the Behavior of 1 and 2.** Although the introduction of the carbonyl groups into the chromophore of this OPV indeed gives rise to a slightly larger value of  $\delta$ , it

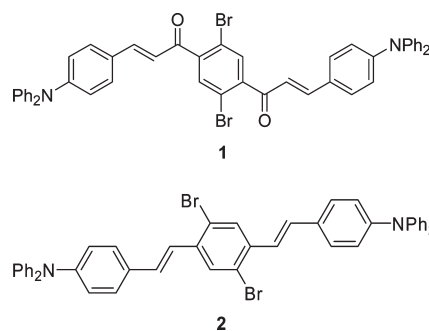


**FIGURE 3.** Structures of the parent dibromo OPV, **2**, and of the corresponding carbonyl-containing analogue, **1**, used to examine one aspect of the two-photon-sensitized production of singlet oxygen.

**TABLE 1.** Photophysical Properties of **1** and **2** in Air-Saturated Toluene

|          | $\Phi_{\text{F}}^a$ | $\Phi_{\text{T}}^b$ | $\Phi_{\text{ic}}^c$ | $f_{\text{T}}^{\text{O}_2^a}$ | $E_{\text{T}}/\text{kJ/mol}$ | $\Phi_{\Delta}^d$ | $\delta(\lambda)^d/\text{GM}$ |
|----------|---------------------|---------------------|----------------------|-------------------------------|------------------------------|-------------------|-------------------------------|
| <b>1</b> | 0.33                | 0.33                | 0.34                 | 0.84                          | 160                          | 0.28              | 1740                          |
| <b>2</b> | 0.44                | 0.44                | 0.12                 | 0.90                          | 148                          | 0.38 <sup>e</sup> | 1310                          |

<sup>a</sup>10% uncertainty. <sup>b</sup>~20% uncertainty. <sup>c</sup>Obtained from the relationship  $\Phi_{\text{ic}} = 1 - \Phi_{\text{T}} - \Phi_{\text{F}}$ . <sup>d</sup>15% uncertainty. Determined at  $\lambda_{\text{max}}$  of the two-photon spectrum, which is 845 nm for **1** and 770 nm for **2** (see Figure 4). <sup>e</sup>We have reported a value of  $0.45 \pm 0.05$  for **2**,<sup>4,7</sup> and the present number, although smaller, is still within our error limits.

does not result in the expected increased yield of singlet oxygen (Table 1). Keeping our overall mechanistic perspective in mind, we performed a series of complementary experiments to help elucidate these observations.

**Quantum Yields.** We first note that, for the triplet state photosensitized production of singlet oxygen,  $\Phi_{\Delta}$  can be expressed as the product of three parameters: the triplet state quantum yield,  $\Phi_{\text{T}}$ , the fraction of triplet states quenched by ground state oxygen,  $f_{\text{T}}^{\text{O}_2}$ , and the fraction of these latter quenching events that result in singlet oxygen production,  $S_{\Delta}$  (eq 1).<sup>3</sup>

$$\Phi_{\Delta} = \Phi_{\text{T}} f_{\text{T}}^{\text{O}_2} S_{\Delta} \quad (1)$$

Like  $\Phi_{\Delta}$ , values of  $\Phi_{\text{T}}$  were measured in independent experiments. Using [O<sub>2</sub>]-dependent changes in the T<sub>1</sub> lifetime, we obtained  $f_{\text{T}}^{\text{O}_2}$ . Details are provided in the Supporting Information. Values of  $S_{\Delta}$  could then be obtained using eq 1.

Although  $f_{\text{T}}^{\text{O}_2}$  for **1** is indeed slightly smaller than that for **2** (Table 1), this difference is not enough to account for the observed difference in  $\Phi_{\Delta}$ . Moreover, the data indicate that, for each molecule,  $S_{\Delta} \sim 1$ . (Using independently established arguments,<sup>3,36</sup> these values of  $S_{\Delta}$  are consistent with the  $E_{\text{T}}$  values of 160 and 148 kJ/mol for **1** and **2**, respectively.) Indeed, carrying this point further, with  $S_{\Delta}$  values of  $\sim 1$  for both **1** and **2**, we hesitate to suggest that the respective T<sub>1</sub> states would have a different amount of CT character. Thus, on the basis solely of the model described in the Introduction, our data already reveal an unexpected result.

Going further, the explanation for the difference in  $\Phi_{\Delta}$  is readily seen in the corresponding values of  $\Phi_{\text{T}}$ ; the yield of the singlet oxygen precursor, the sensitizer triplet state, is smaller in **1** than in **2**. Simply put, in contrast to our expectation, addition of the carbonyl to our chromophore does not result in an increased triplet yield.

(34) Lower, S. K.; El-Sayed, M. A. *Chem. Rev.* **1966**, *66*, 199–241.

(35) Wilkinson, F.; Helman, W. P.; Ross, A. B. *J. Phys. Chem. Ref. Data* **1993**, *22*, 113–262.

(36) Schmidt, R. *Photochem. Photobiol.* **2006**, *82*, 1161–1177.

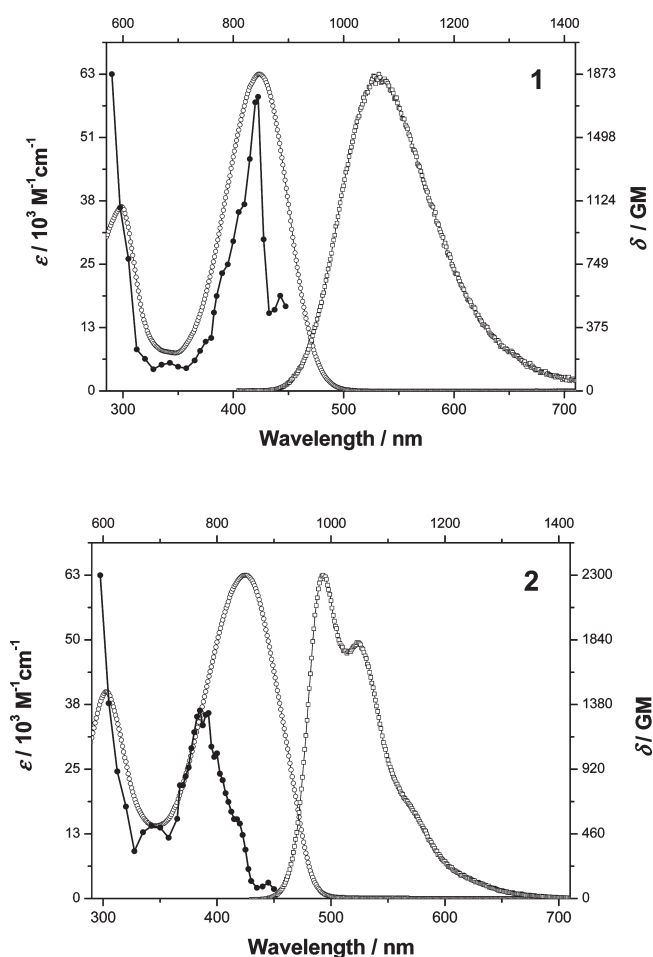


**FIGURE 4.** One-photon absorption (○), two-photon excitation (●), and fluorescence (□) spectra of **1** and **2**, all recorded in toluene. The lower *x*-axis refers to the total transition wavelength, while the upper *x*-axis shows the wavelength used in the two-photon experiments.

Using the relation  $\Phi_{ic} = 1 - \Phi_T - \Phi_F$ , we ascertain that **1** has a much larger quantum yield of internal conversion,  $\Phi_{ic}$ , than does **2** (Table 1). Thus, the lower triplet yield in **1** is principally a consequence of events that better facilitate nonradiative  $S_1 \rightarrow S_0$  coupling in **1**. Among other things, such coupling could arise as a consequence of (1) a greater probability for CT-mediated interaction between the  $S_0$  and  $S_1$  states in **1** than in **2** and/or (2) a larger molecular flexibility of **1** relative to **2** which promotes the transfer of electronic energy to vibrational/rotational degrees of freedom.

In light of this notion of conformational flexibility, it is important to demonstrate that the molecules do not undergo irreversible photoisomerization under the conditions of our experiments. Specifically, photoinduced *cis*–*trans* geometric isomerization is known to occur in stilbene and cinnamic acid derivatives<sup>37–40</sup> and, as such, may influence our data. However, in independent absorption, fluorescence, and <sup>1</sup>H NMR experiments, we ascertained that photoisomerization

(37) Waldeck, D. H. *Chem. Rev.* **1991**, *91*, 415–436.

(38) Lub, J.; Ezquerro, M. P.; Malo, B. *Mol. Cryst. Liq. Cryst.* **2006**, *457*, 161–180.

(39) Saltiel, J. J. *Am. Chem. Soc.* **1968**, *90*, 6394–6400.

(40) Brey, L. A.; Schuster, G. B.; Drickamer, H. G. *J. Am. Chem. Soc.* **1979**, *101*, 129–134.

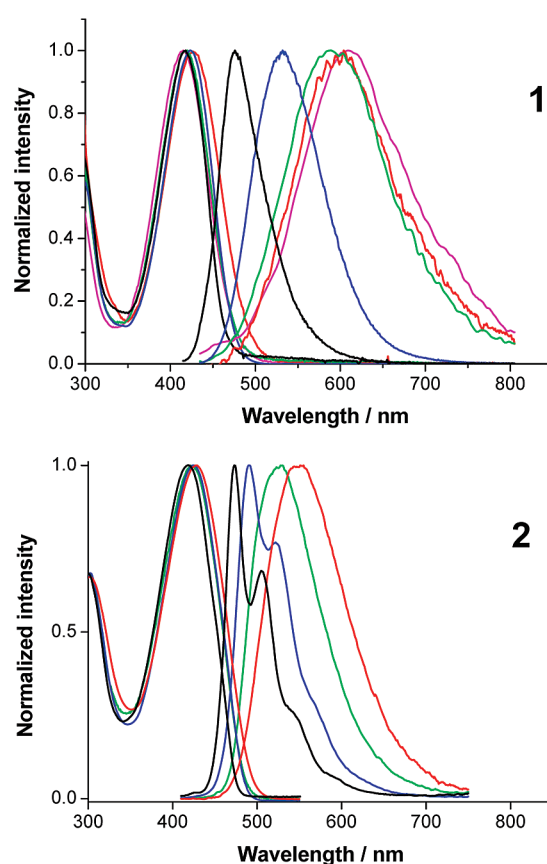


**FIGURE 5.** Solvent-dependent absorption and emission spectra for compounds **1** and **2**. Solvents used: (red) benzonitrile; (magenta) acetonitrile; (green) THF; (black) cyclohexane; (blue) toluene.

does not occur in **1** and **2** under our conditions (see pertinent data in the Supporting Information).

**One-Photon Spectra.** One-photon absorption and fluorescence spectra for **1** and **2** dissolved in toluene are shown in Figure 4. The respective absorption spectra are similar, whereas the fluorescence spectra are distinctly different: the emission profile of **2** has pronounced vibronic structure, whereas the profile of **1** is broadened and structureless. Moreover, the Stokes shift observed for **1** is significantly greater than that for **2**. Although these data are consistent with our suggestion that **1** is more conformationally flexible than **2**, they could also reflect the fact that the emitting state in **1** has more CT character than that of **2**.<sup>25,41</sup>

In an attempt to comment further on the relative amounts of CT character, at least in the emitting state of these molecules, we examined the fluorescence spectra of **1** and **2** in solvents of varying polarity (Figure 5). The results clearly show that, for both molecules, the absorption spectrum is not strongly dependent on the solvent, whereas the emission spectrum red-shifts as the polarity of the solvent is increased. This latter effect is more pronounced for **1**, indicating that this molecule may indeed have more CT character in its solvent-stabilized emitting state than does **2**.

Although the solvent-dependent phenomenon shown in Figure 5 is often described simply in terms of an increase in the amount of CT character in the emitting state,<sup>25,41</sup> a

(41) Suppan, P.; Ghoneim, N. *Solvatochromism*; The Royal Society of Chemistry: Cambridge, 1997.

related model which uses slightly different language can likewise be applied. Specifically, and given the apparent symmetry of these molecules, one could invoke the solvent-dependent “symmetry-breaking” arguments of Terenziani et al.<sup>42</sup> Here, the charge distribution in the excited state is seen to preferentially lose its initial high degree of symmetry due to a dynamic coupling with the solvent (e.g., coupling between the vibrational modes of the excited-state solute and the solvation coordinates). In any event, the net result would be the solvent-dependent introduction of electronic asymmetry in the excited state which, for our purposes, is equivalent to a solvent-dependent “increase in the amount of CT character”.

Finally, it is important to comment on the appearance, or lack thereof, of vibronic structure on the emission profiles. Specifically, in the nonpolar solvents cyclohexane and toluene, where CT character is not expected to play a large role, we see that the emission profile of **1** is structureless whereas that of **2** is not. Under these conditions, the data may now reflect the fact that **1** is more conformationally flexible than **2**.

**Two-Photon Spectra.** In discussing the two-photon spectra shown in Figure 4, we first focus on the marked increase in  $\delta$  observed for both molecules as the transition energy increases (i.e., as the two-photon irradiation wavelength is decreased below  $\sim 700$  nm). This likely reflects the phenomenon of “resonance-enhancement”, which becomes significant as the two-photon excitation wavelength approaches the onset of the one-photon absorption profile.<sup>10,43</sup>

In the spectral range 700–900 nm, both **1** and **2** have a two-photon absorption band with a distinct maximum. At this maximum, in the nominally nonpolar solvent toluene, **1** indeed has a larger value of  $\delta$  than does **2** (Table 1), as we had hoped in the design of our chromophores (vide supra). However, this difference in  $\delta$  values is small and barely exceeds our error limits. The fact that the respective  $\delta$  values are similar implies that there is not an appreciable difference in the extent of CT character in **1** and **2**, at least in toluene. In turn, this implies that the difference in  $\Phi_{\Delta}$  values for **1** and **2** is not due to CT effects but, rather, reflects another phenomenon.

Note that, as plotted in Figure 4, these two-photon absorption bands of **1** and **2** appear narrower than the corresponding lowest energy one-photon absorption bands. This is a consequence of the different wavelength scales used to present the one- and two-photon data, respectively. Any further discussion of the relative band widths, although interesting, becomes potentially complicated because one must consider vibronic contributions to the virtual state, among other things.<sup>21</sup> It is also interesting to note the small peak/shoulder at  $\sim 890$  nm in both two-photon spectra. Although it is possible that this could be an artifact of our experiment, we rather believe that it is a real, but presently unassigned, feature of the spectra. In any event, these aspects of the data do not preclude us from making substantive statements.

For molecule **2**, the distinct two-photon absorption band has  $\lambda_{\max} = 770$  nm (i.e., transition at 385 nm). This band is clearly blue-shifted relative to the most dominant band

in the one-photon spectrum (transition at 425 nm). Selection rules established for two-photon transitions appear to be pertinent in this case. Specifically, in a centrosymmetric molecule, transitions between states with the same parity are allowed for two-photon processes, whereas an excited state with a parity opposite to that of the initial state (e.g., a gerade–ungerade transition) is accessible only through a one-photon transition.<sup>44</sup> Thus, the absorption data obtained for **2** conform to the Jablonski diagram shown in Figure 1 in which the states populated in the one- and two-photon processes are different, and indicate that **2** is a centrosymmetric molecule.

In contrast, the one- and two-photon absorption bands of **1** closely resemble each other, with a transition  $\lambda_{\max}$  of  $\sim 420$  nm. Within the framework of the established selection rules, such spectral coincidence indicates that, unlike **2**, molecule **1** appears to be noncentrosymmetric. Thus, our analysis must clearly go beyond simple static representations of a given molecule, as shown in Figure 3.

In previous reports, we established that, when working with large molecules that have multiple degrees of conformational freedom, care should indeed be exercised when using qualitative symmetry arguments to interpret one- and two-photon spectra.<sup>10</sup> Rather, it is more appropriate to perform a rigorous calculation of one- and two-photon transition probabilities as a function of thermally accessible ground-state geometric conformers. That is, one needs to consider a Boltzmann-weighted average of the energetically accessible conformers.

Using an ab initio computational approach based on response theory,<sup>9,10,28</sup> we have calculated one- and two-photon transition probabilities for both **1** and **2**. The results obtained, shown in the Supporting Information, are consistent with the experimental data shown in Figure 4. We find that when multiple ground-state geometric conformers of **1** are accessible, the one- and two-photon absorption spectra are coincident. The computational results specifically suggest that a noncentrosymmetric ground-state conformer of **1** is readily populated (it is, in fact, calculated to be the lowest energy conformer), and that it contributes to the spectral data. For compound **2**, where the lowest energy ground-state conformer is centrosymmetric, the first allowed two-photon transition always occurs at a higher energy than the first allowed one-photon transition (e.g., see the Jablonski diagram in Figure 1).

Thus, our one- and two-photon spectral data recorded in the nominally nonpolar solvent toluene, along with the associated computations, are consistent with our proposed model in which the differences in the oxygen-dependent photophysics of **1** and **2** derive principally from the fact that molecule **1** appears to be more conformationally flexible than molecule **2**.

**2. Systematic Changes in the Central Moiety of the OPV System.** Given the results in the preceding section, we thought it appropriate to investigate the effects of putting the carbonyl group directly on the central aromatic ring of our OPV system. We also wanted to assess the effects of changing the central aromatic moiety through (1) the addition of functional groups other than a carbonyl and a heavy atom and (2) replacement of the phenyl ring with a larger

(42) Terenziani, F.; Painelli, A.; Katan, C.; Charlot, M.; Blanchard-Desce, M. *J. Am. Chem. Soc.* **2006**, *128*, 15742–15755.

(43) Drobizhev, M.; Karotki, A.; Kruk, M.; Rebane, A. *Chem. Phys. Lett.* **2002**, *355*, 175–182.

(44) McClain, W. M. *Acc. Chem. Res.* **1974**, *7*, 129–135.

**TABLE 2. OPV Derivatives Used to Examine the Effects of Systematic Structural Changes on Selected Photophysical Properties<sup>a</sup>**

|    | X<br>(See Figure 2) | $\lambda_{\text{max}}^{\text{abs}} / \text{nm} (\log \epsilon)$ | $\lambda_{\text{max}}^{\text{em}} / \text{nm}$ | $\delta_{\text{max}} / \text{GM}^b$<br>( $\lambda_{\text{max}}$ ) | $\Phi_{\text{F}}^c$ | $\Phi_{\Delta}^c$ |
|----|---------------------|---|--|---|---------------------|-------------------|
| 3  |                     | 480 (4.61)<br>394 (4.59)<br>347 (4.47)<br>303 (4.63)            | 601  | 2280 <sup>e</sup>   | 0.4                 | 0.15              |
| 4  |                     | 429 (4.79)<br>305 (4.64)  | 516  | 1970<br>(775 nm)  | 0.7                 | 0.17              |
| 5  |                     | 416 (4.87)<br>302 (4.56)  | 475<br>504                                     | 1460<br>(760 nm)  | 0.8                 | 0.09              |
| 6  |                     | 431 (4.65)<br>302 (4.58)  | 556  | 1800<br>(760 nm)  | 0.05                | 0.02              |
| 7  |                     | 419 (4.78)<br>303 (4.76)  | 481<br>511                                     | 1040<br>(775 nm)  | 0.1                 | 0.04              |
| 8  |                     | 454 (4.78)<br>306 (4.60)  | 534  | 4110 <sup>e</sup>   | 0.6                 | 0.06              |
| 9  |                     | 484 (4.49)<br>419 (4.59)<br>303 (4.64)                          | -- <sup>f</sup>                                | -- <sup>f</sup>   | 0.00                | 0.00              |
| 10 |                     | 410 (4.87)<br>306 (4.49)  | 458<br>486                                     | 1150 <sup>e</sup>   | 0.9 <sup>d</sup>    | 0.08              |
| 11 |                     | 428 (4.87)<br>306 (4.55)  | 484<br>513                                     | 1350 <sup>e</sup>   | 0.8                 | 0.11              |
| 12 |                     | 428 (4.90)<br>304 (4.61)  | 486<br>517                                     | 1970<br>(780 nm)  | 0.8                 | 0.09              |
| 13 |                     | 472 (4.87)<br>304 (4.63)  | 531  | 2815<br>(845 nm)  | 0.87                | 0.13              |
| 14 |                     | 409 (4.90)<br>300 (4.62)  | 459<br>481                                     | 2030 <sup>e</sup>   | 0.8                 | 0.08              |
| 15 |                     | 423 (4.83)<br>306 (4.63)  | 480<br>507                                     | 1410<br>(765 nm)  | 0.2                 | 0.13              |

<sup>a</sup>All data reported in this table were recorded in air-saturated toluene. <sup>b</sup>~20% uncertainty. <sup>c</sup>~10% uncertainty. <sup>d</sup>A value of 0.91 reported by Kauffman and Moyna<sup>45</sup> is consistent with our value. <sup>e</sup>In these cases, we did not record a clear and distinct two-photon absorption band maximum (see the Supporting Information). Thus, the absorption cross section reported here likely underestimates the true value. <sup>f</sup>This compound does not fluoresce, nor does it produce singlet oxygen. Thus, a probe based on an optical approach could not easily be used to quantify two-photon absorption.

naphthyl group. The intent was to survey a comparatively large number of compounds and, as such, it was sufficient to only determine values of  $\delta$ ,  $\Phi_{\Delta}$ , and  $\Phi_{\text{F}}$ . On the basis of these

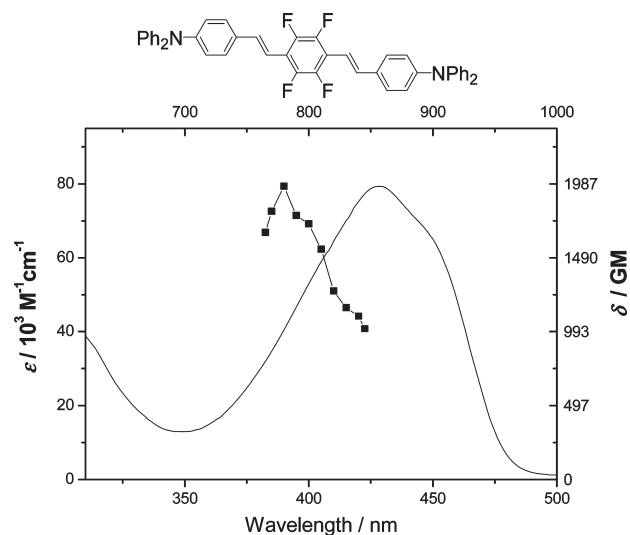


**FIGURE 6.** One-photon absorption (solid line) and two-photon excitation (■) spectra for molecule **12**. The upper x-axis shows the wavelengths used in the two-photon experiment.

parameters, we could readily establish a meaningful picture of features important in the design of OPV-based two-photon singlet oxygen sensitizers. The compounds chosen for this work and the pertinent photophysical parameters obtained are shown in Table 2.

We start by noting that all values of  $\Phi_{\Delta}$  are quite small and are significantly less than those obtained for compounds **1** and **2**. This is particularly of interest for compounds **3–7** where a carbonyl group was directly attached to the central aromatic ring. Thus, the data indicate that, for these OPVs, including carbonyl functionalities in this way does not appear to be as successful a strategy as using a heavy atom to induce intersystem crossing.

With regard to heavy atoms, we note that, in the case of the naphthalene-based sensitizers **14** and **15**, the addition of Br atoms to the central aromatic system indeed appears to have an appreciable influence on the probability of intersystem crossing (i.e.,  $\Phi_{\text{F}}$  for **15** is much smaller than that for **14**). However, this does not translate into an increased yield of singlet oxygen in **15**. This is in contrast to the single-ring phenyl-based sensitizers, where  $\Phi_{\Delta}$  for the dibromo-substituted molecule **2** is appreciably larger than that for the unsubstituted compound **10**. Moreover, the  $\Phi_{\Delta}$  value for the phenyl-based dibromo compound **2** is noticeably larger than that for the naphthyl-based dibromo compound **15**. This latter result may reflect an increased amount of CT character in the naphthyl-based system that adversely affects  $S_{\Delta}$ . In any event, the key conclusion here is that, for these OPVs, replacing the central phenyl-based aromatic moiety with a more extensive naphthyl-based system does not contribute to the desired effect of increasing  $\Phi_{\Delta}$ .

Two-photon excitation spectra were recorded for all compounds. Although the spectra were, in general, not recorded with as high a resolution and/or over as large a wavelength range as those recorded for **1** and **2**, the data are sufficient to yield useful information (see the representative spectrum in Figure 6; all other spectra can be found in the Supporting Information.). For most of the molecules listed in Table 2, we

have clear evidence that, as in the case of molecule **2**, the two-photon spectrum is blue-shifted relative to the one-photon spectrum. Thus, and as we have discussed with respect to **2** in the previous section, the spectroscopic data for these compounds point to ground state populations dominated by a centrosymmetric conformation.

Unlike the values of  $\Phi_{\Delta}$  which are small and essentially substituent-independent, the  $\delta$  values are generally large and respond to the nature of the substituent. This not only confirms that the OPV class of molecules is indeed well-suited for two-photon absorption but that the two-photon transition probability can indeed be sensitive to the functional groups attached to the chromophore. With respect to the latter, it certainly appears that the largest values of  $\delta$  are obtained from molecules in which the central aromatic ring is functionalized with an electron-withdrawing substituent; an observation which is consistent with established electron push–pull arguments.<sup>18,20</sup> As an illustration of this, we find a reasonably good correlation between our  $\delta$  values and the NMR chemical shift of the two aromatic protons on the central ring of our OPVs; the latter parameter reflects the ground-state electron density in this part of the molecule which, in turn, is reflected in the extent to which the protons are shielded (see the Supporting Information for the data).

Given the relative insensitivity of the  $\Phi_{\Delta}$  values to changes in these particular substituents, it is difficult to generalize and quantify the extent of correlation between the two-photon absorption properties and singlet oxygen quantum yields. Nevertheless, it is still useful to look at selected examples where interesting changes of substance are observed. For example, the effects of replacing a formyl with an acetyl group (i.e., molecules **3** and **6**) are arguably larger than what one might expect, certainly in light of the changes observed with other substituents.

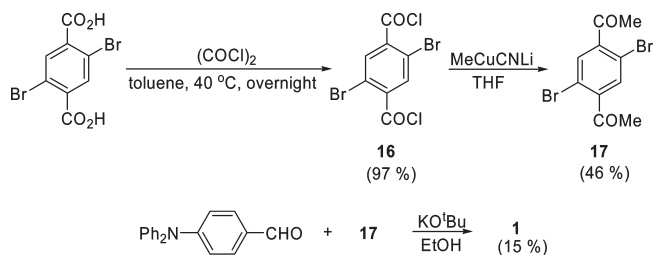
In any event, the data clearly show that, as we established in our more detailed study of molecules **1** and **2**, one should be cautious when trying to look for and apply rule-of-thumb arguments in the development of optimized two-photon singlet oxygen sensitizers. Even for as “simple” a series as the OPVs in Tables 1 and 2, there apparently is still no substitute for an in-depth investigation of the pertinent photophysical properties for a given molecule of interest.

Arguably, one of the more useful conclusions we can make is that none of the molecules in Table 2 are likely to be successful candidates for future applications relying on two-photon induced singlet oxygen production. The  $\Phi_{\Delta}$  values are simply too low, and despite promising  $\delta$  values, the overall product  $\delta\Phi_{\Delta}$  is rather small. This is certainly true in comparison with  $\delta\Phi_{\Delta}$  values reported, for example, for various porphyrin derivatives and porphycenes.<sup>10,17</sup> Although additional efforts may improve values of  $\delta$  in such OPVs, one must be less optimistic about the chance of significantly enhancing the singlet oxygen yield at the same time. On the other hand, the majority of these OPV molecules are good fluorophores and would thus be well-suited for applications based on two-photon induced fluorescence.

## Conclusion

The conscious and methodical design of viable and efficient two-photon singlet oxygen sensitizers is a nontrivial exercise.

## SCHEME 1. General Procedure Used To Prepare **1**



Although a great deal is indeed already known about factors that independently (i) govern singlet oxygen production in a sensitized process and (ii) influence the probability of two-photon absorption, the complexity of the combined two-photon singlet oxygen photosystem still makes simple qualitative predictions untenable.

We have shown that the well-studied OPV structural motif examined herein can provide useful information about structure–property relationships pertinent for a better understanding of two-photon-sensitized singlet oxygen production. However well-suited to nonlinear light absorption, the OPV system is not ideal for the development of molecules optimized for the production of singlet oxygen following two-photon absorption. Although exceptional and suitable compounds may still be found from this class of molecules, a systematic approach to successfully develop two-photon singlet oxygen sensitizers will more likely come from a focus on other classes of organic molecules.

## Experimental Section

**Photophysical Characterization.** Singlet oxygen quantum yields were determined by comparing the intensity of singlet oxygen phosphorescence produced by the molecule under study to that obtained from a standard.<sup>7</sup> In these experiments, a Nd:YAG nanosecond laser was used as the excitation source, and a liquid nitrogen cooled Ge-detector was used to record the time-resolved singlet oxygen phosphorescence decay. Fluorescence and triplet-state quantum yields,  $\Phi_{\text{F}}$  and  $\Phi_{\text{T}}$ , respectively, triplet-state energies,  $E_{\text{T}}$ , and triplet-state quenching parameters were likewise determined using established procedures (see the Supporting Information).

Two-photon excitation spectra, and associated  $\delta$  values, were quantified using methods<sup>7</sup> wherein either the near-IR phosphorescence of singlet oxygen or the sample fluorescence were used as spectroscopic probes (see the Supporting Information). In these approaches, recorded data are compared to those obtained from a reference standard for which the pertinent photophysical parameters have been independently determined.

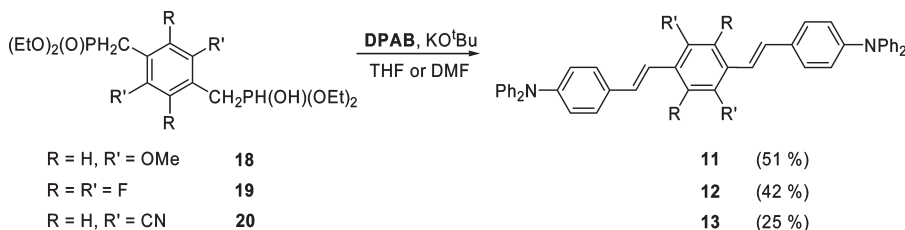
**General Synthetic Strategy.** Important precursors in the synthesis of all compounds were 4-(N,N-diphenylamino)-benzaldehyde, DPAB, and N,N-diphenyl-4-vinylbenzamine; the latter was obtained from DPAB using a published procedure.<sup>46</sup> These compounds were used in either a Horner–Wadsworth–Emmons (HWE) or Heck reaction to yield the “wings” attached to the central aromatic moiety of our OPVs (Figure 2).

Synthesis of **1** was achieved using a Knoevenagel condensation reaction between DPAB and 1-(4-acetyl-2,5-dibromophenyl)ethanone with potassium *tert*-butoxide as the base in ethanol (Scheme 1). A general reason for choosing the diphenylamino end-group is that, for OPVs and related compounds, this moiety has been shown to confer better photostability in comparison with dialkylamino

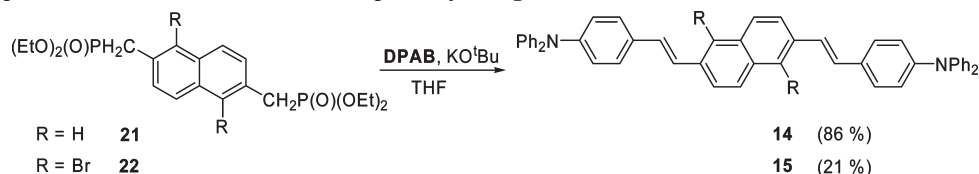
(45) Kauffman, J. M.; Moyna, G. *J. Org. Chem.* **2003**, *68*, 839–853.

(46) Sengupta, S. *Tetrahedron Lett.* **2003**, *44*, 307–310.

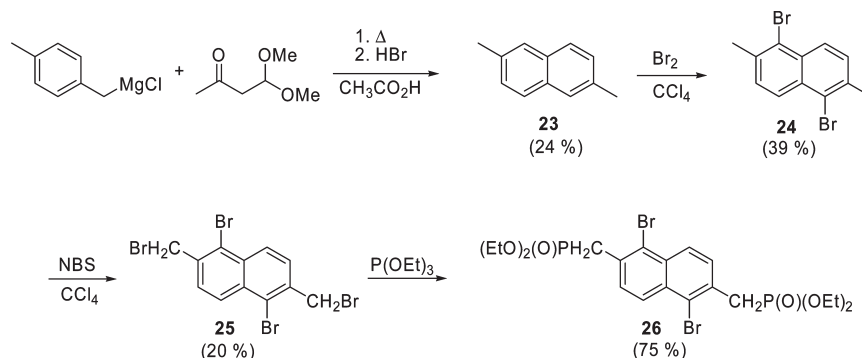
## SCHEME 2. OPV Derivatives Prepared Using the HWE Reaction



## SCHEME 3. Naphthalene-Based OPV Molecules Prepared by Using the HWE Reaction



## SCHEME 4. Synthesis of the Dibromonaphthalene-Based Diposphonate Ester Required for the Preparation of Compound 15



groups.<sup>45</sup> Furthermore, a diarylamino group is a less efficient quencher of singlet oxygen than a dialkyl amino group,<sup>47,48</sup> a phenomenon which can be significant in systems where the local concentration of the sensitizer is high. The synthesis of compounds **2** and **10**, both of which have been published,<sup>4,49</sup> used the same general approach as that shown in Scheme 1.

The HWE reaction was used to prepare compounds **11–13** and is outlined in Scheme 2. The details with respect to compound **13** have been published.<sup>5,19</sup>

The naphthyl-containing OPV compounds were likewise prepared using HWE methodology (Scheme 3). For compound **14**, we used [6-(diethoxyphosphorylmethyl)naphthalen-2-ylmethyl]-phosphonic acid diethyl ester in this procedure. However, for compound **15**, we needed to make a dibromonaphthalene-based phosphonate ester. The synthesis of this compound is shown in Scheme 4. Here, we first prepared 2,6-dimethylnaphthalene in a condensation reaction with *p*-methylbenzylmagnesium chloride and 4,4-dimethoxybutan-2-one. This reaction has previously been described by Kochetkov et al.,<sup>50</sup> where it was claimed that a 3:2 mixture of sulfuric and phosphoric acid was the best choice for final hydrolysis and that the use of HBr resulted in significantly lower yields. However, the 24% yield of 2,6-dimethyl-

naphthalene obtained in the present work using HBr does not deviate significantly from the 27% yield reported by Kochetkov using H<sub>2</sub>SO<sub>4</sub>/H<sub>3</sub>PO<sub>4</sub>. Treatment of the dimethylnaphthalene with Br<sub>2</sub> yielded 1,5-dibromo-2,6-dimethylnaphthalene. Subsequent bromination of the methyl groups with NBS and conversion using the Michaelis–Arbuzov reaction gave the required phosphonate ester needed for the HWE reaction.

The HWE reaction works well with reactants insensitive to basic conditions. However, to incorporate ketones, for example, into the OPV motif, the carbonyl groups need to be protected if a HWE strategy is to be applied. Rather, we decided to use a different approach, the Heck reaction,<sup>51</sup> to accomplish the key coupling step. To this end, we prepared several 2,5-dibromo-substituted benzenes, which were then reacted with *N,N*-diphenyl-4-vinylbenzylamine under Heck conditions as shown in Scheme 5.

One of the most efficient reagents used for the Heck reaction is P(<sup>t</sup>Bu)<sub>3</sub>,<sup>52</sup> but this compound is pyrophoric and must be handled in a glovebox. However, P(<sup>t</sup>Bu)<sub>3</sub> can be generated in situ from the [(<sup>t</sup>Bu)<sub>3</sub>PH]BF<sub>4</sub> salt and a suitable base. We used the method reported by Netherton and Fu<sup>52</sup> where P(<sup>t</sup>Bu)<sub>3</sub> is generated in situ using *N*-cyclohexyl-*N*-methylcyclohexylamine (Cy<sub>2</sub>NMe) as the base. The yields for **3–6** (31–59%) are noticeably larger than those for **7–8** (3–10%) and may reflect the effects of electron withdrawing (methanesulfonyl, nitro) or sterically hindered (*tert*-butyl ketone) groups.

(47) Monroe, B. M. *J. Phys. Chem.* **1977**, *81*, 1861–1864.

(48) Wilkinson, F.; Helman, W. P.; Ross, A. B. *J. Phys. Chem. Ref. Data* **1995**, *24*, 663–1021.

(49) Poulsen, T. D.; Frederiksen, P. K.; Jørgensen, M.; Mikkelsen, K. V.; Ogilby, P. R. *J. Phys. Chem. A* **2001**, *105*, 11488–11495.

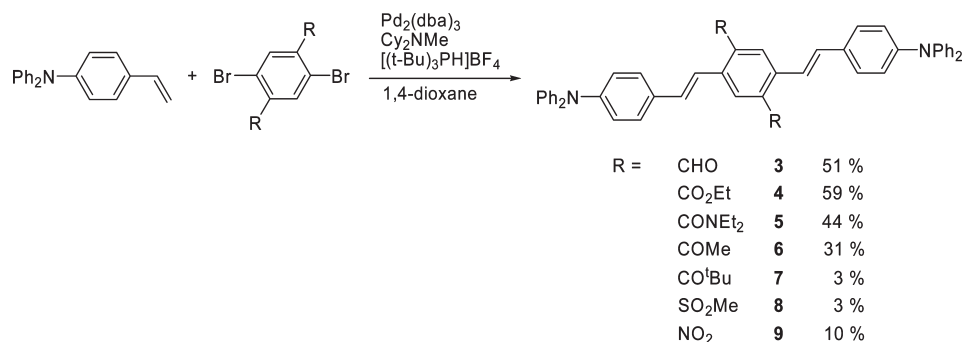
(50) Kochetkov, N. K.; Nifantev, E. E.; Nesmeyanov, A. N. *Dokl. Akad. Nauk SSSR* **1955**, *104*, 422–426.

(51) Heck, R. F.; Nolley, J. P. *J. Org. Chem.* **1972**, *37*, 2320–2322.

(52) Netherton, M. R.; Fu, G. C. *Org. Lett.* **2001**, *3*, 4295–4298.



## SCHEME 5. Preparation of OPV Derivatives Using the Heck Reaction



## Synthesis Details and Characterization of Compounds

**2,5-Dibromoterephthaloyl Dichloride (16, See Scheme 1).**<sup>53</sup>

To a stirred solution of 2,5-dibromoterephthalic acid (7.15 g, 22.1 mmol) in toluene (100 mL) was added (COCl)<sub>2</sub> (6.05 g, 47.7 mmol) along with a few drops of DMF as catalyst. The reaction mixture was stirred overnight at 40 °C, and the solvent was removed under reduced pressure. The isolated crude product was redissolved in toluene (20 mL), and a small amount of CaH<sub>2</sub> was added. The mixture was stirred for 1 h at rt and filtered. Removal of the solvent under reduced pressure left 7.62 g (96%) of the title compound as off-white flakes: <sup>1</sup>H NMR(CDCl<sub>3</sub>, 300 K) 8.20 (s, 2H); <sup>13</sup>C NMR(CDCl<sub>3</sub>, 300 K) 164.3, 139.8, 137.0, 119.3.

**1-(4-Acetyl-2,5-dibromophenyl)ethanone (17, See Scheme 1).**

Methylolithium (1.4 M) in Et<sub>2</sub>O (49 mL, 97 mmol) was added to a slurry of CuCN (7.00 g, 78.2 mmol) in THF (100 mL) at -78 °C under an Ar atmosphere, and the mixture was stirred at this temperature for 1.5 h. Freshly prepared 2,5-dibromoterephthaloyl dichloride (7.17 g, 19.9 mmol) was then added, and the solution was stirred for 40 min at -78 °C. The reaction was quenched at -78 °C by addition of water (150 mL), and the mixture was allowed to warm to rt and then filtered through a pad of Celite. The aqueous layer was then extracted three times with Et<sub>2</sub>O, and the combined organic phases were washed with brine and then dried with MgSO<sub>4</sub>. The solvent was removed under reduced pressure leaving the crude product which was recrystallized from EtOH yielding 2.93 g (46%) of the title compound as white needles: mp 142–144 °C; <sup>1</sup>H NMR (CDCl<sub>3</sub>, 300 K) 7.66 (s, 2H), 2.63 (s, 6H); <sup>13</sup>C NMR(CDCl<sub>3</sub>, 300 K) 198.9, 144.0, 133.7, 117.8, 30.1; HRMS-(EI<sup>+</sup>) *m/z* calcd for C<sub>10</sub>H<sub>8</sub>Br<sub>2</sub>O<sub>2</sub><sup>+</sup> 317.8891, found 317.8883. Anal. Calcd for C<sub>10</sub>H<sub>8</sub>Br<sub>2</sub>O<sub>2</sub>: C, 37.54; H, 2.52. Found: C, 37.96; H, 2.41.

**(*E,E*)-2,5-Dibromo-1,4-bis[3-(4-diphenylaminophenyl)acryloyl]benzene (1).** KO<sup>t</sup>Bu (0.08 g, 0.7 mmol) was added to a solution of 1-(4-acetyl-2,5-dibromophenyl)ethanone (0.55 g, 1.7 mmol) and 4-diphenylaminobenzaldehyde<sup>54</sup> (1.04 g, 3.80 mmol) in EtOH (100 mL), and the reaction mixture was refluxed for 2 h. The reaction mixture was filtered after cooling to rt, and Celite was added. The solvent was removed in vacuo, and the remaining solid was loaded onto a column. Purification by DCVC<sup>55</sup> (petroleum ether (60–80 °C)/

CHCl<sub>3</sub>) and recrystallization from a 1:1 CH<sub>2</sub>Cl<sub>2</sub>/petroleum ether mixture at 60–80 °C yielded 0.22 g (15%) of **1** as a dark yellow powder: mp 217–219 °C; <sup>1</sup>H NMR(CDCl<sub>3</sub>, 300 K, 250 MHz) 7.62 (s, 2H), 7.42 (d, 4H, *J* = 9 Hz), 7.37 (d, 2H, *J* = 10 Hz), 7.34–7.27 (m, 8H), 7.19–7.07 (m, 12H), 7.00 (d, 4H, *J* = 9 Hz), 6.89 (d, 2H, *J* = 16 Hz); <sup>13</sup>C NMR(CDCl<sub>3</sub>, 300 K, 62.5 MHz) 192.9, 151.0, 148.2, 146.5, 143.8, 133.3, 130.2, 129.6, 126.6, 125.8, 124.5, 122.5, 120.9, 118.5. Anal. Calcd for C<sub>48</sub>H<sub>34</sub>Br<sub>2</sub>N<sub>2</sub>O<sub>2</sub>: C, 69.41; H, 4.13; N, 3.37. Found: C, 68.85; H, 4.44; N, 3.22.

**(*E,E*)-2,5-Diformyl-1,4-bis[2-(4'-diphenylaminophenyl)vinyl]benzene (3).** Reaction of Pd<sub>2</sub>(dba)<sub>3</sub> (175 mg, 0.19 mmol), [(*t*-Bu)<sub>3</sub>PH]BF<sub>4</sub> (84 mg, 0.29 mmol), Cy<sub>2</sub>NMe (1.24 g, 6.35 mmol), 1,4-dioxane (50 mL), 2,5-dibromoterephthalaldehyde (0.77 g, 2.64 mmol), diphenyl(4-vinylphenyl)amine (1.56 g, 5.75 mmol), and DCVC (*n*-heptane/1,2-C<sub>2</sub>H<sub>4</sub>Cl<sub>2</sub>) yielded 0.90 g (51%) of the title compound as dark red crystals: mp 238–240 °C; <sup>1</sup>H NMR (CDCl<sub>3</sub>, 300 K) 10.43 (s, 2H), 8.15 (s, 2H), 7.88 (d, 2H, *J* = 16 Hz), 7.45 (d, 4H, *J* = 9 Hz), 7.34–7.26 (m, 6H), 7.19–7.01 (m, 20H); <sup>13</sup>C NMR (CDCl<sub>3</sub>, 300 K) 192.0, 148.4, 147.3, 138.3, 135.3, 134.3, 130.6, 130.3, 129.4, 128.1, 124.9, 123.5, 122.8, 120.8. Anal. Calcd for C<sub>48</sub>H<sub>36</sub>N<sub>2</sub>O<sub>2</sub>·0.125C<sub>2</sub>H<sub>4</sub>Cl<sub>2</sub>: C, 84.58; H, 5.37; N, 4.09. Found: C, 84.64; H, 5.34; N, 4.15.

**(*E,E*)-2,5-Diethoxycarbonyl-1,4-bis[2-(4'-diphenylaminophenyl)vinyl]benzene (4).** Reaction of Pd<sub>2</sub>(dba)<sub>3</sub> (97 mg, 0.11 mmol), [(*t*-Bu)<sub>3</sub>PH]BF<sub>4</sub> (47 mg, 0.16 mmol), Cy<sub>2</sub>NMe (0.63 g, 3.22 mmol), 1,4-dioxane (50 mL), 2,5-dibromoterephthalic acid diethyl ester (0.40 g, 1.05 mmol), diphenyl(4-vinylphenyl)amine (0.63 g, 2.32 mmol), and DCVC (1,2-C<sub>2</sub>H<sub>4</sub>Cl<sub>2</sub>/*n*-heptane) followed by recrystallization of the crude product from a 1:1 mixture CH<sub>2</sub>Cl<sub>2</sub> and EtOH yielded 0.47 g (59%) of the title compound as red needles: mp 223–224 °C; <sup>1</sup>H NMR (CDCl<sub>3</sub>, 300 K) 8.20 (s, 2H), 7.79 (d, 2H, *J* = 16 Hz), 7.43 (d, 4H, *J* = 8 Hz), 7.33–7.21 (m, 8H), 7.16–6.98 (m, 18H), 4.44 (q, 4H, *J* = 7 Hz), 1.44 (t, 6H, *J* = 7 Hz); <sup>13</sup>C NMR (CDCl<sub>3</sub>, 300 K) 167.2, 147.8, 147.5, 137.0, 131.6, 131.4, 129.3, 128.7, 127.8, 124.6, 124.4, 123.4, 123.2, 61.4, 14.4. Anal. Calcd. for C<sub>52</sub>H<sub>44</sub>N<sub>2</sub>O<sub>4</sub>·0.125-CH<sub>2</sub>Cl<sub>2</sub>: C, 81.15; H, 5.78; N, 3.63. Found: C, 81.52; H, 5.65; N, 3.65.

**(*E,E*)-2,5-Diethylaminocarbonyl-1,4-bis[2-(4'-diphenylaminophenyl)vinyl]benzene (5).** The general procedure for the Heck reaction was followed, with 5 days of reflux instead of overnight: Pd<sub>2</sub>(dba)<sub>3</sub> (132 mg, 0.15 mmol), [(*t*-Bu)<sub>3</sub>PH]BF<sub>4</sub> (71 mg, 0.24 mmol), Cy<sub>2</sub>NMe (0.80 g, 4.09 mmol), 1,4-dioxane (50 mL), 2,5-dibromo-*N,N,N',N'*-tetraethylterephthalamide (0.95 g, 2.19 mmol), and diphenyl(4-vinylphenyl)amine (1.21

(53) Lamba, J. J. S.; Tour, J. M. *J. Am. Chem. Soc.* **1994**, *116*, 11723–11736.

(54) Wang, X.-M.; Zhou, Y.-F.; Yu, W.-T.; Wang, C.; Fang, Q.; Jiang, M.-H.; Lei, H.; Wang, H.-Z. *J. Mater. Chem.* **2000**, *10*, 2698–2703.

(55) Pedersen, D. S.; Rosenbohm, C. *Synthesis* **2001**, *16*, 2431–2434.

g, 4.43 mmol). After the quenched reaction mixture was filtered through a plug of silica, it was allowed to stand at rt for 2 days. The precipitate was filtered yielding 0.34 g (44%) of the title compound as yellow needles: mp 257–258 °C; <sup>1</sup>H NMR (CDCl<sub>3</sub>, 300 K) 7.53 (s, 2H), 7.36–7.21 (m, 12H), 7.15–6.99 (m, 18H), 6.94 (d, 2H, *J* = 16 Hz), 4.00–3.74 (bm, 2H), 3.51–3.27 (bm, 2H), 3.15 (q, 4H, *J* = 7 Hz), 1.32 (t, 6H, *J* = 7 Hz), 1.02 (t, 6H, *J* = 7 Hz); <sup>13</sup>C NMR (CDCl<sub>3</sub>, 300 K) 170.1, 147.9, 147.4, 136.5, 133.0, 130.8, 129.3, 127.6, 124.7, 123.3, 123.1, 122.9, 122.1, 42.9, 39.0, 14.0, 13.0. Anal. Calcd for C<sub>56</sub>H<sub>54</sub>N<sub>4</sub>O<sub>2</sub>·0.5C<sub>4</sub>H<sub>8</sub>O<sub>2</sub>: C, 81.09; H, 6.80; N, 6.52. Found: C, 80.71; H, 6.46; N, 6.69.

**(*E,E*)-2,5-Diacetyl-1,4-bis[2-(4'-diphenylaminophenyl)vinyl]benzene (6).** Reaction of Pd<sub>2</sub>(dba)<sub>3</sub> (112 mg, 0.12 mmol), [(*t*-Bu)<sub>3</sub>PH]BF<sub>4</sub> (63 mg, 0.22 mmol), Cy<sub>2</sub>NMe (0.74 g, 3.8 mmol), 1,4-dioxane (50 mL), 1-(4-acetyl-2,5-dibromophenyl)ethanone (0.37 g, 1.2 mmol), diphenyl(4-vinylphenyl)amine (0.70 g, 2.6 mmol), and DCVC (1,2-C<sub>2</sub>H<sub>4</sub>Cl<sub>2</sub>/*n*-heptane) (2 times) followed by recrystallization of the crude product from a 1:1 mixture of CH<sub>2</sub>Cl<sub>2</sub> and EtOH yielded 0.25 g (31%) of the title compound as a red powder: mp 249–251 °C; <sup>1</sup>H NMR (CDCl<sub>3</sub>, 300 K): 7.86 (s, 2H), 7.49–7.36 (m, 6H), 7.32–7.25 (m, 8H), 7.15–7.09 (m, 8H), 7.09–7.01 (m, 8H), 6.98 (d, 2H, *J* = 16 Hz), 2.65 (s, 6H); <sup>13</sup>C NMR (CDCl<sub>3</sub>, 300 K) 202.1, 148.0, 147.4, 139.8, 135.4, 132.0, 130.9, 129.3, 127.8, 127.0, 124.7, 123.9, 123.3, 123.2, 30.3. Anal. Calcd for C<sub>50</sub>H<sub>40</sub>N<sub>2</sub>O<sub>2</sub>·0.33CH<sub>2</sub>Cl<sub>2</sub>: C, 82.91; H, 5.62; N, 3.84. Found: C, 82.70; H, 5.58; N, 3.77.

**(*E,E*)-2,5-Di-*tert*-butylcarbonyl-1,4-bis[2-(4'-diphenylaminophenyl)vinyl]benzene (7).** The general procedure for the Heck reaction was followed, with 5 days of reflux instead of overnight: Pd<sub>2</sub>(dba)<sub>3</sub> (118 mg, 0.13 mmol), [(*t*-Bu)<sub>3</sub>PH]BF<sub>4</sub> (79 mg, 0.28 mmol), Cy<sub>2</sub>NMe (0.73 g, 3.7 mmol), 1,4-dioxane (50 mL), 1-[2,5-dibromo-4-(2,2-dimethylpropionyl)phenyl]-2,2-dimethylpropan-1-one (0.70 g, 1.7 mmol), diphenyl(4-vinylphenyl)amine (0.95 g, 3.5 mmol), and DCVC (*n*-heptane/1,2-C<sub>2</sub>H<sub>4</sub>Cl<sub>2</sub>) (2 times) and recrystallization of the crude product from a mixture of CH<sub>2</sub>Cl<sub>2</sub> and *n*-heptane yielded 0.04 g (3%) of the title compound as a yellow powder: mp 276–277 °C; <sup>1</sup>H NMR (CDCl<sub>3</sub>, 300 K) 7.37 (s, 2H), 7.35–7.21 (m, 14H), 7.16–6.99 (m, 18H), 6.93 (d, 2H, *J* = 16 Hz), 6.78 (d, 2H, *J* = 16 Hz), 1.28 (s, 18H).

**(*E,E*)-2,5-Dimethylsulfonyl-1,4-bis[2-(4'-diphenylaminophenyl)vinyl]benzene (8).** The general procedure for the Heck-reaction was followed, with 3 days of reflux instead of overnight: Pd<sub>2</sub>(dba)<sub>3</sub> (103 mg, 0.11 mmol), [(*t*-Bu)<sub>3</sub>PH]BF<sub>4</sub> (59 mg, 0.20 mmol), Cy<sub>2</sub>NMe (0.69 g, 3.5 mmol), 1,4-dioxane (50 mL), 1,4-dibromo-2,5-bis-methanesulfonylbenzene (0.49 g, 1.3 mmol), diphenyl(4-vinylphenyl)amine (0.70 g, 2.6 mmol), and DCVC (*n*-heptane/1,2-C<sub>2</sub>H<sub>4</sub>Cl<sub>2</sub>) (2 times) and recrystallization of the crude product from a 5:1 mixture CH<sub>2</sub>Cl<sub>2</sub> and EtOH yielded 0.03 g (3%) of the title compound: mp > 300 °C; <sup>1</sup>H NMR (CDCl<sub>3</sub>, 300 K) 8.47 (s, 2H), 7.88 (d, 2H, *J* = 16 Hz), 7.45 (d, 4H, *J* = 8 Hz), 7.35–7.23 (m, 10H), 7.19–7.02 (m, 16H), 3.13 (s, 6H). Anal. Calcd for C<sub>48</sub>H<sub>40</sub>N<sub>2</sub>O<sub>4</sub>S<sub>2</sub>·0.25H<sub>2</sub>O: C, 74.15; H, 5.25; N, 3.60. Found: C, 73.98; H, 5.31; N, 3.59.

**(*E,E*)-2,5-Dinitro-1,4-bis[2-(4'-diphenylaminophenyl)vinyl]benzene (9).** The general procedure for the Heck-reaction was followed, with 3 days of reflux instead of overnight: Pd<sub>2</sub>(dba)<sub>3</sub> (105 mg, 0.11 mmol), [(*t*-Bu)<sub>3</sub>PH]BF<sub>4</sub> (67 mg, 0.23 mmol), Cy<sub>2</sub>NMe (0.67 g, 3.4 mmol), 1,4-dioxane (50 mL), 1,4-dibromo-2,5-bisnitrobenzene (0.45 g, 1.4 mmol), diphenyl-

(4-vinylphenyl)amine (0.74 g, 2.7 mmol), DCVC (*n*-heptane/1,2-C<sub>2</sub>H<sub>4</sub>Cl<sub>2</sub>) (2 times) and recrystallization of the crude product from a mixture of CH<sub>2</sub>Cl<sub>2</sub> and *n*-heptane yielded 0.10 g (10%) of the title compound: mp 221–222 °C; <sup>1</sup>H NMR (CDCl<sub>3</sub>, 300 K) 8.26 (s, 2H), 7.41 (d, 4H, *J* = 9 Hz), 7.35–7.24 (m, 10H), 7.21–7.01 (m, 18H); <sup>13</sup>C NMR (CDCl<sub>3</sub>, 300 K) 149.2, 149.1, 147.1, 135.4, 131.7, 129.4, 129.2, 128.4, 125.2, 123.8, 123.6, 122.4, 118.1. Anal. Calcd. for C<sub>46</sub>H<sub>34</sub>N<sub>4</sub>O<sub>4</sub>·0.25CH<sub>2</sub>Cl<sub>2</sub>: C, 76.30; H, 4.78; N, 7.70. Found: C, 76.15; H, 4.65; N, 8.02.

**[4-(Diethoxyphosphorylmethyl)-2,5-dimethoxybenzyl]phosphonic Acid Diethyl Ester<sup>56</sup> (18, See Scheme 2).** 1,4-Dimethoxy-2,5-bis-bromomethylbenzene (3.67 g, 11.3 mmol) was refluxed in P(OEt)<sub>3</sub> (100 mL) for 2 h. The reaction mixture was concentrated by distilling off excess P(OEt)<sub>3</sub>. Filtering of the product from the cooled concentrated reaction mixture yielded 4.22 g (85%) of white crystals: <sup>1</sup>H NMR (CDCl<sub>3</sub>, 300 K) 6.90 (s, 2H), 4.01 (p, 8H, *J* = 7 Hz), 3.78 (s, 6H), 3.20 (d, 4H, *J* = 20 Hz), 1.22 (t, 12H, *J* = 7 Hz); <sup>13</sup>C NMR (CDCl<sub>3</sub>, 300 K) 151.0 (d, *J*<sub>PC</sub> = 4 Hz), 119.4 (d, *J*<sub>PC</sub> = 5 Hz), 114.0, 61.7 (d, *J*<sub>PC</sub> = 7 Hz), 56.1, 26.4 (d, *J*<sub>PC</sub> = 140 Hz), 16.2 (d, *J*<sub>PC</sub> = 6 Hz).

**(*E,E*)-2,5-Dimethoxy-1,4-bis[2-(4'-diphenylaminophenyl)vinyl]benzene (11).** Potassium *tert*-butoxide (0.55 g, 4.9 mmol) was added to a stirred solution of 1,4-dimethoxy-2,5-bis-bromomethylbenzene (0.57 g, 1.3 mmol) and 4-diphenylaminobenzaldehyde (0.73 g, 2.67 mmol) in THF (100 mL) under an argon atmosphere. The solution was stirred at rt for 45 min and quenched with water. The product precipitated from the quenched reaction mixture and was isolated by filtration: yield 0.45 g (51%); yellow powder; mp 233–234 °C; <sup>1</sup>H NMR (DMSO, 300 K) 7.51 (d, 4H, *J* = 9 Hz), 7.41–7.21 (m, 14H), 7.15–7.03 (m, 12H), 6.99 (d, 4H, *J* = 9 Hz), 3.90 (s, 6H); <sup>13</sup>C NMR (CDCl<sub>3</sub>, 300 K) 151.5, 147.6, 147.2, 132.3, 129.3, 128.3, 127.4, 126.7, 124.4, 123.7, 123.0, 121.8, 109.1, 56.4. Anal. Calcd for C<sub>48</sub>H<sub>40</sub>N<sub>2</sub>O<sub>2</sub>·0.5H<sub>2</sub>O: C, 84.06; H, 6.03; N, 4.08. Found: C, 84.18; H, 5.91; N, 4.10.

**[4-(Diethoxyphosphorylmethyl)-2,3,5,6-tetrafluorobenzyl]phosphonic Acid Diethyl Ester (19, See Scheme 2).** This compound was a gift from Dr. Frederik C. Krebs (Risø) and was prepared according to a published procedure.<sup>57</sup>

**(*E,E*)-2,3,5,6-Tetrafluoro-1,4-bis[2-(4'-diphenylaminophenyl)vinyl]benzene (12).** Potassium *tert*-butoxide (0.50 g, 4.7 mmol) was added to a stirred solution of [4-(diethoxyphosphorylmethyl)-2,3,5,6-tetrafluorobenzyl]phosphonic acid diethyl ester (0.44 g, 0.89 mmol) and 4-diphenylaminobenzaldehyde (0.55 g, 2.01 mmol) in DMF (80 mL) under an argon atmosphere. The solution was stirred under reflux for 30 min and cooled to rt followed by quenching with water. The product precipitated from the quenched reaction mixture and was filtered, recrystallized from toluene, purified by DCVC (*n*-heptane/CHCl<sub>3</sub>), and then recrystallized from benzene: yield 0.26 g (42%); mp > 250 °C; <sup>1</sup>H NMR (CDCl<sub>3</sub>, 300 K) 7.49–7.35 (m, 6H), 7.32–7.22 (m, 10H), 7.17–7.00 (m, 14H), 6.95 (d, 2H, *J* = 17 Hz); <sup>13</sup>C NMR (CDCl<sub>3</sub>, 300 K) 148.7, 147.5, 130.9, 129.4, 127.9, 125.0, 123.6, 123.0; <sup>19</sup>F NMR (CDCl<sub>3</sub>, 330 K) –141.7. Anal. Calcd. for C<sub>46</sub>H<sub>32</sub>F<sub>4</sub>N<sub>2</sub>·0.5H<sub>2</sub>O: C, 79.18; H, 4.77; N, 4.01. Found: C, 79.18; H, 4.55; N, 3.88.

(56) Brehm, I.; Hinneschiedt, S.; Meier, H. *Eur. J. Org. Chem.* **2002**, 3162–3170.

(57) Krebs, F. C.; Jensen, T. *J. Fluorine Chem.* **2003**, 120, 77–84.

**(*E,E*)-2,6-Bis[2-(4'-diphenylaminophenyl)vinyl]naphthalene (14).** Prepared as outlined above for **11** and **12**. The product precipitated from the quenched reaction mixture and was isolated by filtration: yield 2.40 g (86%); yellow powder; mp 226–228 °C; <sup>1</sup>H NMR (CDCl<sub>3</sub>, 300 K) 7.83–7.66 (m, 6H), 7.44 (d, 4H, *J* = 9 Hz), 7.37–7.33 (m, 10H), 7.20–7.00 (m, 18H); <sup>13</sup>C NMR (CDCl<sub>3</sub>, 300 K) 147.6, 147.4, 135.1, 133.2, 131.6, 129.3, 128.4, 128.3, 127.4, 127.1, 126.0, 124.6, 124.0, 123.6, 123.1. Anal. Calcd. for C<sub>50</sub>H<sub>38</sub>N<sub>2</sub>·0.5H<sub>2</sub>O: C, 88.86; H, 5.82; N, 4.14. Found: C, 89.02; H, 5.77; N, 4.00.

**(*E,E*)-1,5-Dibromo-2,6-bis[2-(4'-diphenylaminophenyl)vinyl]naphthalene (15).** Prepared as outlined above for **11** and **12**. The product was recrystallized from toluene and then from CHCl<sub>3</sub>: yield 0.06 g (21%); yellow powder; mp 269–271–115 °C; <sup>1</sup>H NMR (CDCl<sub>3</sub>, 300 K) 8.32 (d, 2H, *J* = 9 Hz), 7.85 (d, 2H, *J* = 9 Hz), 7.66 (d, 2H, *J* = 16 Hz), 7.49 (d, 4H, *J* = 9 Hz), 7.35–7.26 (m, 6H), 7.19–7.02 (m, 20H). Anal. Calcd for

C<sub>50</sub>H<sub>36</sub>N<sub>2</sub>Br<sub>2</sub>·0.33CHCl<sub>3</sub>: C, 69.94; H, 4.24; N, 3.24. Found: C, 69.93; H, 4.09; N, 3.14.

**Acknowledgment.** This work was funded by the Danish National Research Foundation through a block grant for The Center for Oxygen Microscopy and Imaging.

**Supporting Information Available:** Determination of  $\Phi_F$ ,  $\Phi_T$ ,  $E_T$ , and triplet state quenching parameters; determination of two-photon excitation spectra and absorption cross sections,  $\delta$ ; absorption and fluorescence spectra of **1** and **2** before and after irradiation; <sup>1</sup>H NMR spectra of **1** and **2** before and after irradiation; computational methods and results; one- and two-photon spectra for compounds **3–15**; plot of the two-photon absorption cross section against the NMR chemical shift of selected protons; pertinent <sup>1</sup>H and <sup>13</sup>C NMR spectra for compounds **1–17**. This material is available free of charge via the Internet at <http://pubs.acs.org>.